Zeitschrift: IABSE reports of the working commissions = Rapports des commissions de travail AIPC = IVBH Berichte der Arbeitskommissionen

Band: 11 (1971)

Rubrik: Prepared discussion

DISCUSSION PRÉPARÉE / VORBEREITETE DISKUSSION / PREPARED DISCUSSION

A Comparison between the Theoretical Values and the Experimental Results for the Ultimate Shear Strength of Plate Girders

Comparaison des valeurs théoriques et des résultats expérimentaux pour la résistance à la ruine des poutres à âme pleine soumises au cisaillement

Vergleich der theoretischen Werte und der Versuchsergebnisse für die Tragfähigkeit schubbeanspruchter Blechträger

TOKIO FUJII
Dr. Chief Research Engineer, Research Inst.
Ishikawajima-Harima Heavy Industries Co., Ltd. Japan

1. Preface

In this report the results of comparison between the theoretical values by Fujii's formula and the following experimental results are presented in relation to the ultimate shear strength of plate girders.

(A) Homogeneous mild steel symmetrical plate girders by Basler et al.[1], Rodkey and Škaloud[10], Škaloud[9], and Fujii[8].

(B) Homogeneous high tension steel symmetrical plate girders by Cooper et al.[2], Konishi et al.[3], Okumura and Nishino[4], and Okumura et al.[5].

(C) Hybrid symmetrical plate girders by Carskaddan[6] and Höglund[7].

(D) Unsymmetrical plate girders by Ostapenko et al.[6]

(E) Longitudinally stiffened plate girders by Patterson et al.[12] and Komatsu[11].

An electronic computor FACOM 230-25 was used for the calculation of theoretical values and the results are summerized in Table 1.

2. Consideration

2.1 Homogeneous mild steel symmetrical plate girders

Theoretical values against the experiments by Basler et al.[1]

---

* Research Institute of Ishikawajima-Harima Heavy Industries Co., Ltd.

are calculated following the formulation in the report [13] and the errors are within the range of ± 6%. The numerical results show a little change from the values reported in the 8th Congress of IABSE [14]. The reason for this is due to the calculation of the shear buckling coefficient k_s, which was formerly estimated from the figure by interpolation.

For the experiments by Rockey et al.[10], the pure ultimate shear force gave comparatively high values to the experimental values especially for the girders with flexible flanges. Then, the ultimate shear forces are calculated again including the effect of bending moment. The results show good coincidence with the test results except GT6 and GT6' girders. The experimental correlations between the flange rigidity and the ultimate shear force are graphically shown in their report [10]. The theoretical values are added in those figures for the purpose of comparison and are shown in Fig. 1 (a). (b), and (c). It seems that the theory well explains the test results.

For the experiments reported in this Colloquium by Škaloud[9], the theoretical shear forces agree well with the experimental results except TG5, & 5' which have strong flanges. In this case, theoretical values including bending effect gave rather low values. The comparison is also shown graphically in Fig. 2.

In Fujii's experiment[8], the girders were tested almost fixed at the both ends. The theoretical values including the bending effect agree with the test results.

2.2 Homogeneous high tension steel symmetrical plate girders.

Cooper's experiments[2] were carried out using the 80K high tension steel plate girders. In this case theoretical values are a little higher than the experimental values. This difference is considered to be due to the bending effect.

For the experiments by Konishi et al.[3], the theoretical value shows a good agreement with the test result. The same coincidences are noticed for the experiments by Okumura et al.[4][5]

2.3 Hybrid symmetrical plate girders

The theoretical values are calculated against the experiments by Carskaddan[6]. The good coincidence is obtained except C-AC2 Girder.

Höglund has reported the experiments[7] on plate girders without vertical stiffeners. For this case, the theoretical formula is reduced by assuming the panel aspect ratio being infinity ($\lambda = \infty$) as follows,

$$V_u = \nu_u V_p = \frac{2\nu_{cr}}{1 + \nu_{cr}^2} V_p$$

where V_p = plastic shear force

$\nu_{cr} = \tau_{cr} / \tau_{wr}$

τ_{wr} = web yielding stress (shear)

τ_{cr} = web buckling stress (shear)

The theoretical loads against the experiments by Höglund are obtained by using the average shear force of the buckled web, as follows.

Pu = Vu/4 for B1, B4, and Pu = Vu/2.5 for K1.

The calculated values show good coincidence with the test results of B1 and K1, but there is large difference between the two in case of B4.

2.4 Unsymmetrical plate girders.

Ostapenko had performed the experiments on unsymmetrical plate girders[6]. The theoretical values are calculated two cases for each test girder. In the first case, the effect of rigidity of flanges is estimated from the scantling of upper flange and in the second case from the lower flange. There are large differences between the two numerical values and the experimental values are near to the later values. Ostapenko had shown good coincidence between his theoretical values and the experimental ones.

2.5 Longitudinally stiffened plate girders.

For these girders, the theoretical values are obtained by

summing up the ultimate shear strength of each panel subdivided by longitudinal stiffeners. The effect of flange rigidity for each panel is assumed as follows,

for upper panel : upper flange,
for middle panel : assume very large value,
for lower panel : lower flange.

The theoretical values compared with the experimental results by Komatsu[11] and Patterson[12] are shown in Table 1. They show comparatively good results.

The experiments on longitudinally stiffened plate girders had been performed by Ostapenko[12] and Cooper[12]. The author abstained to compare the theoretical values with these test result because the bending effect was considerably large in these cases and the formulation of interactive effect has not been established for longitudinally stiffened plate girders.

3. Conclusion

In Fujii's theory, the beam mechanism, in which the central plastic hinge is assumed arising at the midspan of the flanges between the vertical stiffeners, is used for the estimation of the effect of the flange rigidity on the ultimate shear force.

This assumption does not agree with the experimental results observed for the girders with very flexible flanges and with very strong flanges.

For the girders with flexible flanges, the effect of the flange rigidity becomes small, and the theoretical values agree well with the test results as shown in the report. So it is considered that there is no need to modify the theory. For the girders with very strong flanges, the effect of the flange rigidity becomes large, and the frame mechanism which was introduced by Ostapenko should be considered. This will make it possible to analyze the ultimate shear strength of the unsymmetrical plate girders.

References

(1) K. Basler, B. Thürliman and others: "Web Buckling Tests on Welded Plate Girders"
Bulletin No.64 Welding Research Council, N.Y., 1960.

(2) P.B. Cooper and others: "Welded Constructional Alloy Steel Girders"
Proc. of ASCE ST1, 1964

(3) I. Konishi and others: "Theories and Experiments on the Load Carrying Capacity of Plate Girders"
Report of Research Committee of Bridges, Steel Frames and Welding in Kansai District in Japan, July 1965

(4) T. Okumura and others: "Failure Tests of Plate Girders using Large sized Models"
Structural Engineering Laboratory Report, Department of Civil Engineering, Univ. of Tokyo, 1966

(5) T. Okumura and others: "Failure Test on Plate Girders"
Structural Engineering, Univ. of Tokyo, 1967

(6) C. Chern and A. Ostapenko: "Ultimate Strength of Plate Girders under Shear"
Fritz Engineering Laboratory Report No.328.7,Aug. 1969

(7) T. Höglund: "Simply Supported Long Thin Plate I-Girders Without Web Stiffeners Subjected to Distributed Transverse Load"
IABSE Colloquium on Design of Plate Girders for Ultimate Strength, March, 1971.

(8) F. Sakai, T. Fujii and Y. Fukuchi: "Review on Experiments of Plate Girders"
JSSC Vol. 4, No.27 1968 (In Japanese)

(9) M. Škaloud: "Ultimate Load and Failure Mechanism of Web of Large Width-to-Thickness Ratios, Subjected to Shear and Attached to Flanges of Various Flexural Rigidities"
IABSE Colloquium on Design of Plate Girders for Ultimate Strength. March, 1971.

(10) K. Rockey and M. Škaloud: "Influence of the Flexural Rigidity of Flanges upon the Load-Carrying Capacity and Failure Mechanism of Webs in Shear"
ACTA TECHNICA CSAV No.3 1969

(11) S. Komatsu: "Ultimate Strength of Stiffened Plate Girders Subjected to Shear"
IABSE Colloquium on Design on Plate Girders for Ultimate Strength. March, 1971

(12) A. Ostapenko and C. Chern: "Strength of Longitudinally Stiffened Plate Girders under Combined Loads"
Fritz Engineering Laboratory Report No. 328.10 Dec. 1970

(13) T. Fujii, Y. Fukumoto, F. Nishino and T. Okumura: "Research Works on Ultimate Strength of Plate Girders and Japanese Provisions on Plate Girder Design"
IABSE Colloquium on Design of Plate Girders for Ultimate Strength. March, 1971

(14) T. Fujii: "On an improved theory for Dr. Basler's theory"
Prel. Publication of 8th Congress IABSE, 1968

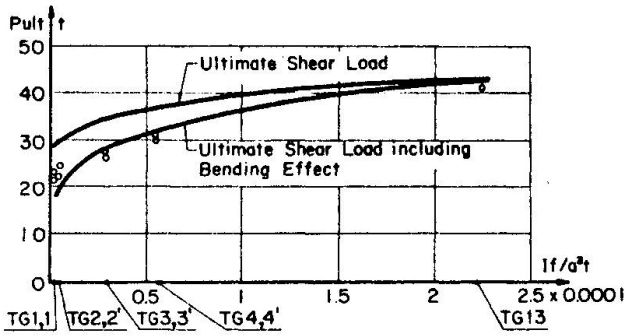

Fig. 1 (a) Comparison between the Experimental Values (α=1.0) by Rockey[10] and the Theoretical Values by Fujii

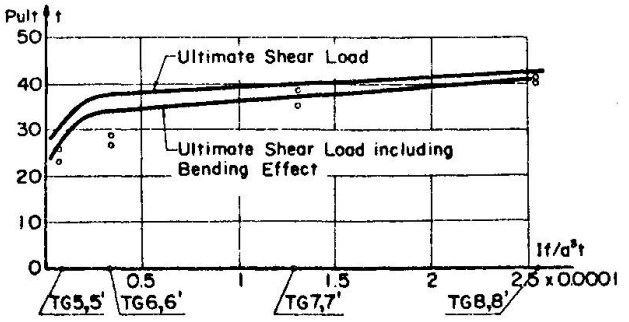

Fig. 1 (b) Comparison between the Experimental Values (α=1.5) by Rockey[10] and the Theoretical Values by Fujii

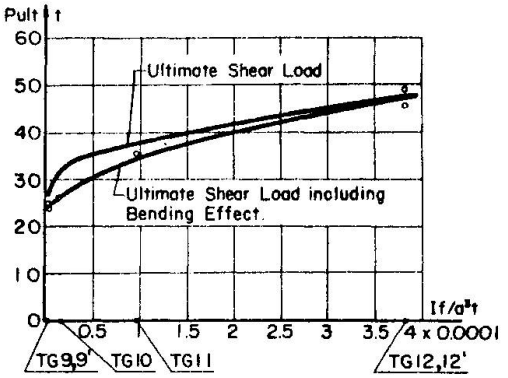

Fig. 1 (c) Comparison between the Experimental Values (α=2.0) by Rockey[10] and the Theoretical Values by Fujii

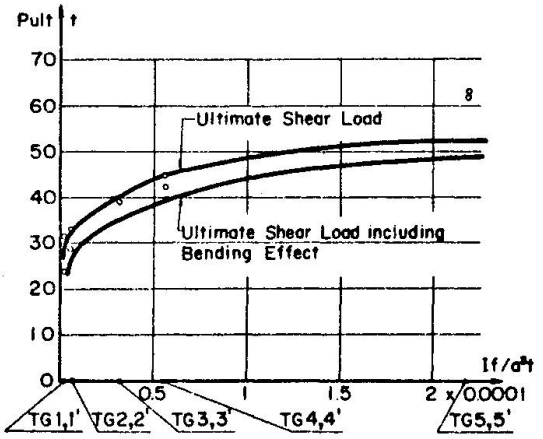

Fig. 2 Comparison between the Experimental Values (α=1.0) by Škaloud[9] and the Theoretical Values by Fujii

Table-1 Summary of the comparison between the experimental values and the theoretical values by Fujii

Author & Source	Girder No.	hw / tw	Aspect Ratio	Web		Upp. Flange		Low Flange		Vu^{ex}	Calculated Value						$\frac{Vu^{ex}}{Vu^{F}}$
				hw x tw	σwy	b_f x t_f	σfy	b_f x t_f	σfy		ϵ	ks	ν_{cr}	ν_{uo}	ν_u	Vu^F	
				in. x in.	ksi.	in. x in.	ksi.	in. x in.	ksi.	kips							
Basler et al.[1]	G6-T1	259	1.5	50x0.193	36.7	12.13x0.778	39.7	Symmetry		116	0.056	10.87	0.239	0.453	0.608	110.4	1.05
	G6-T2	"	0.75	"	"	"	"			150	0.223	15.09	0.332	0.598	0.874	157.5	0.95
	G6-T3	"	0.5	"	"	"	"			177	0.503	27.8	0.592	0.876	1.00	179.8	0.98
	G7-T1	255	1.0	50x0.196	"	12.19x0.768	37.6			140	0.120	12.28	0.279	0.517	0.744	136.5	1.03
	G7-T2	"	"	"	"	"	"			145	0.120	12.28	0.279	0.517	0.744	136.5	1.06
	G8-T1	254	3.0	50x0.197	38.2	12.00x0.750	41.3			85	0.013	9.56	0.211	0.403	0.455	88.4	0.96
	G9-T1	282	"	50x0.131	445	12.00x0.750	41.8			48	0.017	9.56	0.080	0.159	0.298	45.6	1.05
	G9-T2	"	1.5	"	"	"	"			75	0.069	10.87	0.091	0.180	0.485	72.9	1.03
Cooper et al.[2]	H1-T1	127	3.0	50x0.393	108.1	18.06x0.980	106.4	Symmetry		630	0.015	9.56	0.296	0.545	0.585	641.6	0.98
	H1-T2	"	1.5	"	"	18.06x0.980 17.03x0.982	106.4 105.8			769	0.120	10.87	0.337	0.605	0.789	859	0.90
	H2-T1	128	1.0	50x0.390	110.2	18.06x1.006 17.09x1.008	105.5 108.8			917	0.284	12.28	0.368	0.648	0.927	1018	0.90
	H2-T2	"	0.5	"	"	"				1125	1.137	27.8	0.700	0.939	1.00	1096	1.03
				cm x cm	t/cm^2	cm x cm	t/cm^2	cm x cm	t/cm^2	ton						ton	
Konishi et al.[3]	B	267	1.0	120x0.45	5.00	24.0x1.2	5.00	Symmetry		76	0.043	12.28	0.131	0.258	0.552	75.9	1.00
Okumura & Nishino[4]	G1-1	182	3.0	120x0.66	4.96	25x2.3	5.10	Symmetry		99	0.013	9.56	0.221	0.422	0.469	95.8	1.03
	G1-2	"	1.5	"	"	25x2.3 25x1.3	5.10 4.60			129	0.066	10.87	0.252	0.473	0.635	128.5	1.00
	G2-1	144	3.0	95x0.66	"	25x1.9	5.30			98	0.014	9.56	0.353	0.628	0.658	105.4	0.93
	G2-2	"	1.5	"	"	25x1.9 25x1.3	5.30 4.60			125	0.081	10.87	0.402	0.692	0.802	127.9	0.98

Continued

Okumura et al.[5]	G1	55	2.61	44x0.8	4.40	16x3.0	4.20	Symmetry		82	0.104	9.73	0.910	0.996	1.00	82.7	0.99
	G2	"	"	"	"	20x3.0	"			84	0.130	9.73	0.910	0.996	1.00	82.7	1.02
	G3	70	2.63	56x0.8	"	16x3.0	"			99	0.063	9.72	0.854	0.988	0.996	103.5	0.96
	G4	"	3.57	"	"	25x3.0	"			97	0.054	9.40	0.849	0.987	0.995	103.3	0.94
	G5	"	2.68	"	"	"	"			107	0.095	9.69	0.853	0.988	0.999	103.7	1.03
	G6	"	1.25	"	"	"	"			120	0.438	11.46	0.876	0.991	1.00	103.8	1.16
	G7	"	2.68	"	"	"	"			107	0.095	9.69	0.853	0.988	0.999	103.7	1.03
	G9	90	2.78	72x0.8	"	25x3.0	"			118	0.054	9.65	0.757	0.962	0.979	129.3	0.91
				in. x in.	ksi.	in.x in.	ksi.	in. x in.	ksi.	kips						kips	
Ostapenko et al.[6]	UG1.1	300	0.8	36.0x0.120	44.4	8.0x0.625	34.2	8.0x0.625 10.5x0.750	34.2	88.8	*4 0.559 (0.193)	14.1 (")	0.191 (")	0.369 (")	0.968 (0.758)	94.5 (74.4)	0.94 (1.19)
	UG2.1	295	1.2	36.0x0.122	43.2	8.0x0.625	36.7	8.0x0.625 10.0x0.750	36.7	76	0.273 (0.093)	11.6 (")	0.167 (")	0.326 (")	0.865 (0.610)	83.6 (59.5)	0.91 (1.28)
	UG3.1	295	1.6	36.0x0.122	43.5	8.0x0.625	33.3	8.0x0.625 10.5x0.750	33.3	65.5	0.138 (0.047)	10.69 (")	0.153 (")	0.299 (")	0.640 (0.503)	62.8 (49.7)	1.04 (1.32)
	UG4.1	414	1.77	48.0x0.116	56.1	10.0x0.750	34.1	13.0x1.384	34.1	81.6	0.145 (0.033)	10.43 (")	0.059 (")	0.117 (")	0.571 (0.374)	92.6 (61.9)	0.88 (1.32)
	UG4.6	263	1.77	48.0x0.183	35.5	13.0x1.384	34.1	10.0x0.750	34.1	98.8	0.105 (0.033)	10.43 (2)	0.232 (")	0.440 (")	0.696 (0.551)	110 (89.3)	0.90 (1.12)
Carskaddan[6]	C-AC2	143	5.5	17.88x0.12	30.6	3.67x0.38	109.3	Symmetry		26.7	0.013	9.17	0.658	0.919	0.926	31.1	0.86
	C-AC3	71	"	17.93x0.25	36.5	5.51x0.51	108.0			89.2	0.014	9.17	0.906	0.995	1.00	84.1	1.06
	C-AC4	102	"	17.93x0.17	33.6	5.27x0.64	113.2			55	0.035	9.17	0.812	0.979	0.987	52.3	1.05
	C-AC5	103	"	17.96x0.17	33.6	5.18x0.75	113.6			52.4	0.048	9.17	0.811	0.979	0.989	52.8	0.99
	C-AH1	69	"	17.96x0.26	48.4	5.57x1.0	105.9			130	0.038	9.17	0.884	0.992	0.997	119	1.09

Continued

Author & Source	Girder No.	hw / tw	Aspect Ratio	Web		Upp. Flange		Low. Flange		Vu^{ex}	Calculated Value						$\frac{Vu^{ex}}{Vu^{F}}$
				hw x hw	σwy	b_f x t_f	σfy	b_f x t_f	σfy	(Pu^{ex})	ϵ	ks	ν_{cr}	ν_{uc}	ν_u	Vu^F	
				cm x cm	t/cm^2	cm x cm	t/cm^2	cm x cm	t/cm^2	ton							
Höglund[7]	B1	210	–	60.0x0.286	4.185	22.6x0.99	2.944			3.25	–	8.98	0.185	0.358	0.358	*1 3.34	0.97
	B4	300	–	60.0x0.200	2.80	15.1x0.61	3.04	Symmetry		1.58	–	8.98	0.135	0.265	0.265	*1 1.15	1.37
	K1	210	–	60.0x0.286	4.185	22.6x0.99	2.944			5.28	–	8.98	0.185	0.358	0.358	*1 5.35	0.99
Fujii[8]	S-1	50	3.62	16.0x0.32	3.42	10.0x1.04	2.77			9.2	0.065	9.29	0.939	0.966	1.00	*2 9.12	0.99
	S-2	100	1.82	31.9x0.32	3.59	10.0x1.05	2.78	Symmetry		16.4	0.060	10.37	0.772	0.967	0.985	*2 16.6	0.99
	S-3	149	1.21	47.7x0.32	3.23	10.1x1.05	2.77			20.2	0.072	11.57	0.591	0.876	0.925	*2 19.8	1.02
Škaloud[9]	TG1	400	1.0	100x0.25	2.037	16.0x0.517	2.86			30.9	0.019	12.28	0.143	0.280	0.538	27.6	1.11
	TG1′	〃	〃	〃	〃	〃	〃			23.7	〃	〃	〃	〃	〃	〃	0.86
	TG2	〃	〃	〃	〃	20.0x1.01	2.86			32.6	0.091	〃	〃	〃	0.610	31.6	1.03
	TG2′	〃	〃	〃	〃	〃				28.3	〃	〃	〃	〃	〃	〃	0.90
	TG3	〃	〃	〃	〃	20.0x1.646	2.86	Symmetry		38.8	0.242	〃	〃	〃	0.761	39.6	0.98
	TG3′	〃	〃	〃	〃	〃				38.7	〃	〃	〃	〃	〃	〃	0.98
	TG4	〃	〃	〃	〃	20.0x2.016	2.86			44.6	0.364	〃	〃	〃	0.859	44.7	1.00
	TG4′	〃	〃	〃	〃	〃				42.2	〃	〃	〃	〃	〃	〃	0.94
	TG5	〃	〃	〃	〃	25.0x2.971	2.86			62.9	0.991	〃	〃	〃	1.00	52.5	1.20
	TG5′	〃	〃	〃	〃	〃				61.2	〃	〃	〃	〃	〃	〃	1.17
				in. x in.	t/cm^2	in. x in.	t/cm^2	in. x in.	t/cm^2	ton						ton	
Rockey[10] & Škaloud	TG1	225	1.0	24x0.107	1.595	4.0x0.1875	*3 (1.595)			22.6	0.018	12.28	0.371	0.652	0.715	18.2	1.24
	TG1′	〃	〃	〃	〃	〃	〃			24	〃	〃	〃	〃	〃	〃	1.32
	TG2	225	〃	〃	〃	4.0x0.25	〃			25.2	0.033	〃	〃	〃	0.729	18.7	1.35
	TG2′	〃	〃	〃	〃	〃	〃			23.5	〃	〃	〃	〃	〃	〃	1.25
	TG3	222	〃	24x0.108	〃	4.0x0.5	〃	Symmetry		28.5	0.130	〃	〃	〃	0.826	29.6	0.96
	TG3′	〃	〃	〃	〃	〃	〃			27	〃	〃	〃	〃	〃	〃	0.91
	TG4	225	〃	24x0.107	〃	4.0x0.65	〃			31.8	0.204	〃	〃	〃	0.883	32.0	0.99
	TG4′	〃	〃	〃	〃	〃	〃			30.3	〃	〃	〃	〃	〃	〃	0.95
	TG13	233	〃	24x0.103	1.83	4.0x1.0	(1.83)			41.7	0.534	〃	0.308	0.562	0.987	45.0	0.93
	TG5	233	1.5	〃	〃	8.0x0.375	〃			23.4	0.067	10.87	0.272	0.507	0.658	27.4	0.85
	TG5′									26.0	〃	〃	〃	〃	〃	〃	0.95

Continued

	TG6	233	〃	〃	〃	8.0x0.625	〃	Symmetry		28.4	0.185	〃	〃	〃	0.803	33.6	0.85
	TG6′									26.7	〃	〃	〃	〃	〃	〃	0.80
	TG7	233	〃	〃	〃	{8.0x0.625 / 7.0x0.375}	〃			35.5	0.244	〃	〃	〃	0.852	36.7	0.97
	TG7′									38.6	〃	〃	〃	〃	〃	〃	1.05
	TG8	233	〃	〃	〃	{8.0x0.625 / 7.0x0.625}	〃			40.3	0.348	〃	〃	〃	0.915	41.5	0.97
	TG8′									41.4	〃	〃	〃	〃	〃	〃	1.00
	TG9	233	2.0	24x0.104	18.3	8.0x0.375	(1.83)			24.55	0.038	10.17	0.255	0.478	0.581	24.4	1.01
	TG9′	〃	〃	〃	〃	〃				24.05	〃	〃	〃	〃	〃	〃	0.99
	TG10	235	〃	〃	〃	8.0x0.625	〃	Symmetry		25.7	0.104	〃	〃	〃	0.695	25.8	1.00
	TG11	233	〃	〃	〃	{8.0x0.625 / 6.0x0.625}	〃			35.5	0.183	〃	〃	〃	0.787	34.0	1.04
	TG12	233	〃	〃	〃	{9.0x0.75 / 8.0x0.625 / 7.0x0.5}	〃			45.7	0.313	〃	〃	〃	0.887	47.0	0.97
	TG12′	〃	〃	〃	〃					49.2	〃	〃	〃	〃	〃	〃	1.05

										Longitudinal Stiffener				Vu^{ex}	Vu^F	$\frac{Vu^{ex}}{Vu^F}$
										Number	bs x ts	σsy	hi			
											cm x cm	t/cm²	cm	ton	ton	
(11) Komatsu	A-1	209	0.478	67x0.333	4.534	12.5x1.0	3.783			1			32	56.5	51.3	1.10
	A-2	225	0.480	75x0.333	4.233	12.5x1.0	3.784			1			36	57.5	53.5	1.07
	A-3	225	0.48	75x0.333	4.235	12.5x1.0	3.756	Symmetry		2			24	59.0	53.6	1.10
	A-4	249	0.481	83x0.333	4.395	12.5x1.0	3.738			1			40	63.0	60.4	1.04
	A-5	249	0.481	83x0.333	4.238	12.5x1.0	3.738			2			27	63.5	59.3	1.07
				in. x in.	ksi	in. x in.	ksi	in. x in.	ksi		in. x in.	ksi	in.	psi	psi	
(12) Patterson et al.	F11-T1	365	1.39	95x0.260	34.2	14.16x1.259	24.7			1	4.5x0.5	34.2	19.0	260	261	1.00
	F11-T2	〃	1.20	〃	〃	〃	〃	Symmetry		1	〃	〃	〃	247	274	0.90
	F11-T3	〃	1.00	〃	〃	〃	〃			1	〃	〃	〃	279	292	0.96

*1 Theoretical Ultimate Loads (Pu^F) are calculated as follows.

$Pu^F = Vu^F/4$ for B1, B4, and $Pu^F = Vu^F/2.5$ for K1 Girder

*2 Including the bending effect.

*3 Assumed.

*4 No bracket: effect of flange rigidity is estimated from the lower flange.
bracketed: effect of flange rigidity is estimated from the upper flange.

Leere Seite
Blank page
Page vide

Prepared Discussion in Regard to the Ultimate Load Behaviour of Webs in Shear

Discussion préparée concernant le comportement à la ruine des âmes soumises au cisaillement

Vorbereitete Diskussion zum Traglastverhalten schubbeanspruchter Stehbleche

M. ŠKALOUD
Doc., C.Sc., Ing.
Senior Research Fellow
Czechoslovak Academy of Sciences
Institute of Theoretical and Applied Mechanics
Prague, Czechoslovakia

Introductory Remarks

Some of the 'failed' test girders of the research project described in /1/ were tested once more in the upside-down position. This was decided in the hope that the diagonal plastic buckled pattern which formed in the first test would beneficially affect the wave pattern developing during the second test and perpendicular to the first one.

The test results are included in the final report /2/, which will appear shortly.

The main observations can be summarized as follows:

Buckled Pattern of the Web

The buckled pattern of a web panel of 'failed' girder TG 5' tested once more in the upside-down position is shown in Fig. 1. Fig. 1a shows the girder before the test, and Fig. 1b relates to the final stage of the test in the upside-down position, showing the buckled surface of the web shortly before the failure of the girder.

The process of web buckling is as follows:

In the first stage the new buckled pattern is governed by the wave pattern resulting from the first test and being perpendicular to the new one; therefore, the newly developing diagonal half-waves have to overcome the effect of the

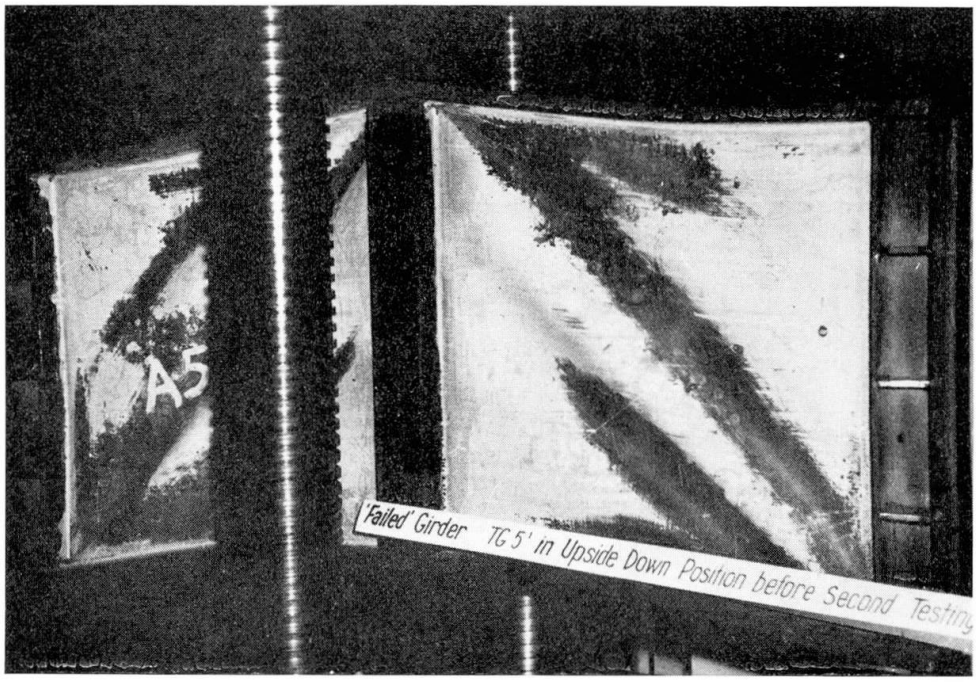
A5
'Failed' Girder 'TG 5' in Upside Down Position before Second Testing

Fig. 1a

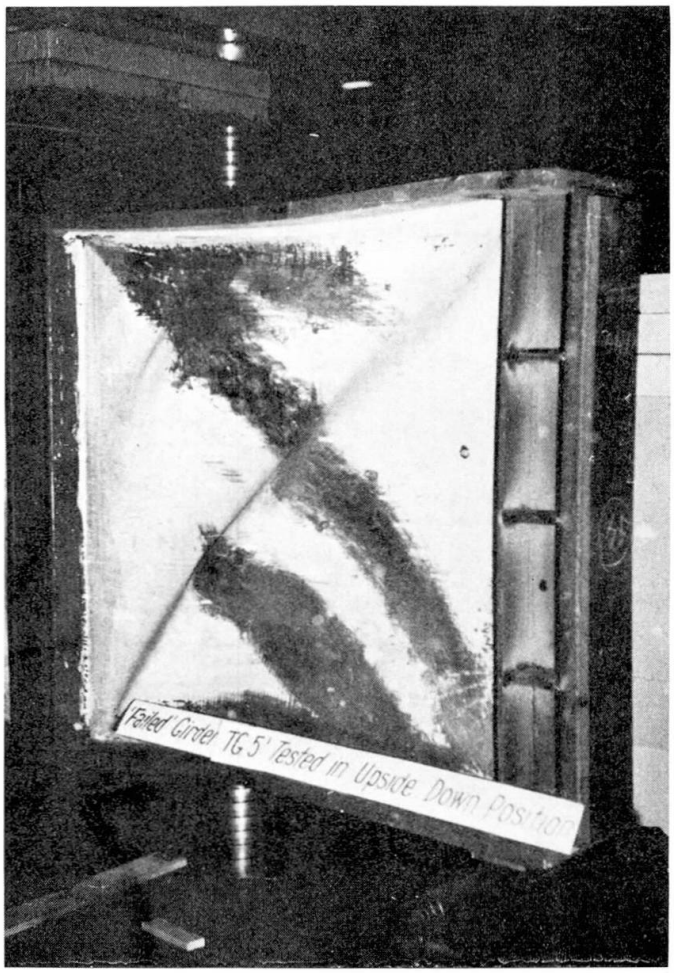
'Failed' Girder 'TG 5' Tested in Upside Down Position

Fig. 1b

perpendicular waving, which, in a sense, stiffens the web. In other words, the diagonal middle plane stresses forming during the upside-down test have to make the web again more or less plane; and only then can the new diagonal buckled pattern form and grow monotonously up to the collapse of the girder.

Deflection of the Girder

The deflection of a girder tested in the upside-down position is shown in Fig. 2, in comparison with the deflection of the same girder tested earlier in the normal position.

It can be seen there that the process of deformation can be divided into three stages.

In the first one, the web is stiffened by the waving which formed in the first test; therefore, the deflection y_{II} of the girder grows fairly slowly, and is less than that which developed in the first test (y_I).

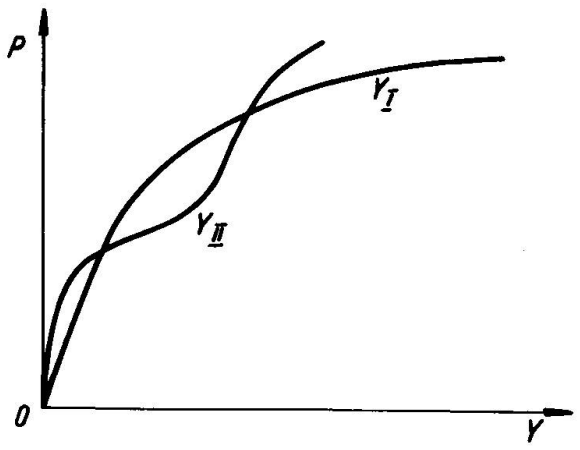

Fig. 2.

In the second stage, during which the buckled pattern of the web changes rapidly from the original deformation to the new diagonal wave pattern, the rigidity of the web (and, accordingly, also that of the whole girder) is substantially lessened. Therefore, the rate of deflection considerably enlarges.

In the third stage, the new buckled pattern (and the corresponding stabilizing effect of membrane stresses) predominates, the behaviour of the girder again stabilizes, and the growth of the girder deflection slows down. The deflection then increases monotonously up to the failure of the girder. This final stage is similar to the performance of the original girder tested in the normal position.

Ultimate Load

The ultimate loads P_{ult}^{II} of failed girders TG 1', TG 3' and TG 5', tested once more in the upside-down position, are listed in Table 1, and compared to the load-carrying capacities P_{ult}^{I} of the same girders obtained in the first test.

An analysis of the table shows that the ratio P_{ult}^{II}/P_{ult}^{I} depends on the flexural rigidity of flanges. The ultimate strength P_{ult}^{II} of girder TG 1', the flanges of which were very flexible, was lower than the load-carrying capacity P_{ult}^{I}. On the other hand, the ultimate loads P_{ult}^{II} of girders TG 3' and TG 5', having rigid flanges, were as high as those in the first test. More accurately, the 'failed girder TG 3' was able to sustain in the second test practically the same load as it did in the first test, it which it still operated as a new girder, delivered from a steel structure plant. 'Failed' girder TG 5', which had very heavy flanges, sustained, when tested once more in the upside-down position, a load that was higher than the load-carrying capacity P_{ult}^{I} of the same girder in the virgin' state. Consequently, the 'failed' girder tested in the upside-down position behaved better than the original one.

Conclusion

The aforementioned information can be regarded only as preliminary. Further evidence in this line is necessary. None the less, having analysed the afore said results, Professor Faltus and the author are inclined to believe that a procedure

Table 1

Girder	I_f/a^3t Units of 10^{-6}	P^{I}_{ult} tons	P^{II}_{ult} tons
TG 1'	0.762	23.7	11.8
TG 3'	29.55	38.7	38.3
TG 5'	218.5	61.18	63.5

similar to that which is mentioned above could be used to 'prestress' web panels in shear, and thereby improve the behaviour of the whole girder. The procedure would consist in subjecting the girder to a load which would induce in the web a slight plastic buckled pattern perpendicular to that which is anticipated to occur under service load.

Of course, the plastic residues in the webs of girders TG 1', TG 3' and TG 5', which developed in an up-to-failure test, were too large. The prestressing buckled pattern would have to be limited to an extent of being just able to create the beneficial diagonal waving, its ordinates being, however, small enough to have no disturbing aesthetical (and psychological) effect.

References:

/1/ Škaloud, M.: Ultimate load and failure mechanism of thin webs in shear. Paper presented at the IABSE Symposium "Design of Plate and Box Girders for Ultimate Strength". London, March, 1971.

/2/ Škaloud, M. and Zörnerová, M.: Post-buckled behaviour of webs in shear, attached to flanges of various flexural rigidities. Czechoslovak Academy of Sciences - Institute of Theoretical and Applied Mechanics 1971.

Das überkritische Verhalten von Aluminium-Vollwandträgern mit Quersteifen (II. Bericht (1971) aus der "Versuchsanstalt für Stahl, Holz und Steine", Universität Karlsruhe)

Post-Critical Behaviour of Aluminium Plate Girders with Transverse Stiffeners (2nd Report 1971)

Comportement post-critique des poutres à âme pleine en aluminium, munies de raidisseurs transversaux (2ème rapport 1971)

O. STEINHARDT
Prof.Dr.-Ing., Dr.sc.techn.h.c.

W. SCHRÖTER
Dipl.-Ing., Wiss.Ass.

Karlsruhe, BRD

Zur Weiterentwicklung des unter Punkt 6 (A) des I. Karlsruher Versuchsberichtes angedeuteten Berechnungsansatzes wurde der in Bild 12 dargestellte 6-feldrige symmetrische Vollwandträger mit zwei unterschiedlichen Gurtquerschnitten (als Träger 6 A und 6 B) untersucht. (Auf die Mehrfeldrigkeit sollte hierbei größerer Wert gelegt werden, da bei nur 2 Feldern die Lasteintragungspunkte in Trägermitte und die Lastabtragungspunkte an den Auflagern natürliche Störzonen enthalten.)

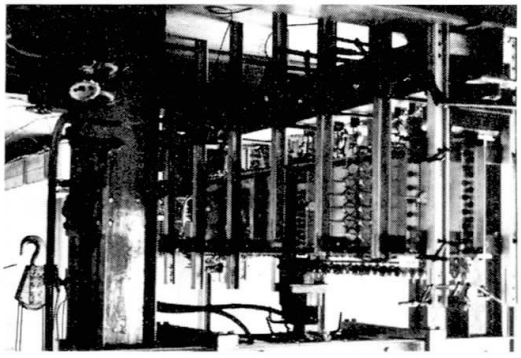

Bild 12a: Versuchsträgeraufbau

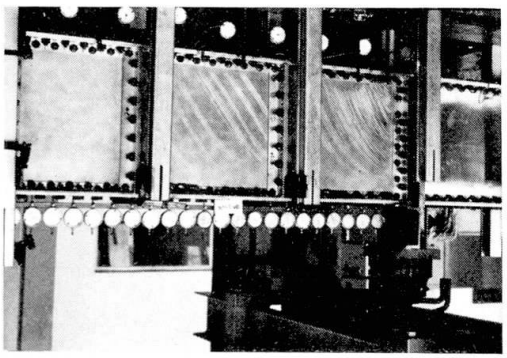

Bild 12b: Reißlackfiguren

Es wurden folgende Abmessungen gewählt: Stützweite l = 2800 mm, Stegblechhöhe b = 450 mm, Stegblechdicke t = 2,0 mm, Stegblechverhältnis α = a/b = 1, Pfostenquerschnitte 2 L 40·40·3 mit Futter ⌀ 40x10, Gurtquerschnitt (Träger 6 A) 2 ⌀ 70·5 bzw. Gurtquerschnitt (Träger 6 B) 1 ⌀ 70·5 mit jeweils 2 L 30·30·3, wobei der am Steg anliegende Schenkel zur Verminderung des Gurtträgheitsmomentes zwischen den HV-Schrauben (M12) jeweils eingesägt war. Weiterhin erfolgte, entsprechend dem 1. Schritt des theoretischen Ansatzes, ein Anschluß der Zwischenpfosten nur an den Gurten. Als Material für die Gurte und Pfosten kam wieder AlMgSi0,5 (F22) und für den Steg AlMg3 (F23) zur Anwendung. An der einen Trägerhälfte wurden geometrische Verformungen gemessen, sowie anhand von Reißlackfiguren erste Angaben über den Verlauf der Spannungstrajektorien ermittelt. In dem mittleren Stegfeld der zweiten Hälfte waren im Bereich der Gurte und in diagonaler Anordnung Dehnungsmeßstreifen angebracht, um Spannungen zu ermitteln.

Für den Träger 6 A ergab sich die theoretische Beullast (für allseitig gelenkige Lagerung der Stegränder) $P_{Kr}^{theor.}$ = 1,75 Mp und aus dem Versuch eine elastische Grenzlast P_{Gr}^{el} = 7,5 Mp, die zu einem überkritischen Bereich ($n^+ = P_{Gr}^{el}/P_{Kr}^{theor.}$ = 4,3) führen. – Für den Träger 6 B ergeben sich die entsprechenden Werte: $P_{Kr}^{theor.}$ = 1,38 Mp, P_{Gr}^{el} = 7,0 Mp, (n^+ = 5,1). Den Verlauf der Beulfiguren und die dazugehörigen Beultiefen in [mm] im Stegfeld II für die drei Laststufen P = 2 Mp, 4 Mp, 7 Mp gibt das Bild 13 wieder.

In Fortsetzung der theoretischen Untersuchungen für einen geeigneten Berechnungsansatz, der das Wechselspiel zwischen Stegdehnung und Gurtverformung für den Querkraft-Anteil Q^{++} aufhellen soll, erfolgt nach Bild 14 eine vereinfachte Betrachtung eines Vollwandträgers mit Stegblech ohne Befestigung an den Zwischensteifen ("Fall A"): Hierbei wird als Belastung für die Gurte der Ansatz

$$q(x) = q_o + q_1 \cdot \left(1 - 2 \cdot \sin^2 \frac{\pi \cdot x}{a}\right) \qquad (1)$$

gewählt. Die Normalkräfte können in diesem Zusammenhang, wie aus Vergleichsrechnungen hervorging, ihres geringen Anteiles wegen unberücksichtigt bleiben. Mit der bekannten Beziehung $EJv^{IV}(x) = q(x)$ und

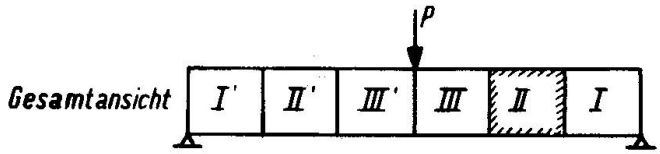

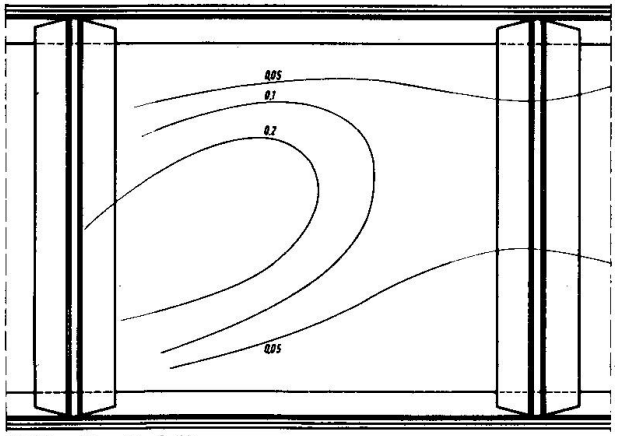

Bild 13a: Träger 6A, P=2Mp

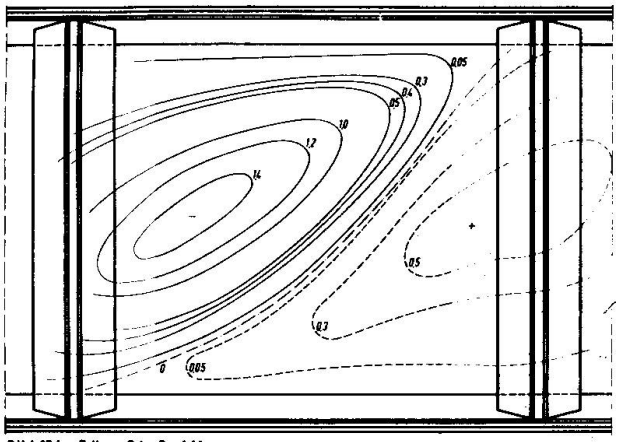

Bild 13b: Träger 6A, P=4Mp

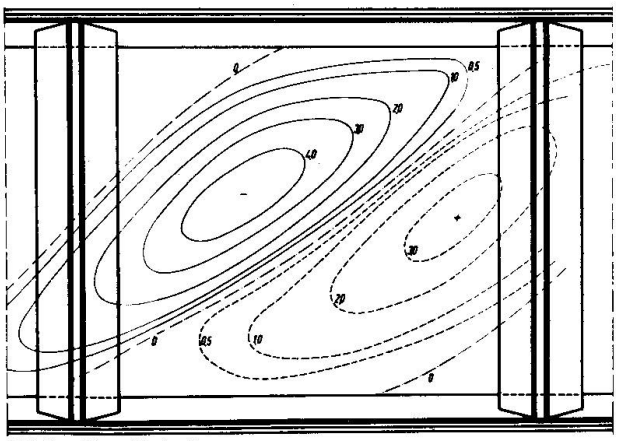

Bild 13c: Träger 6A, P=7Mp

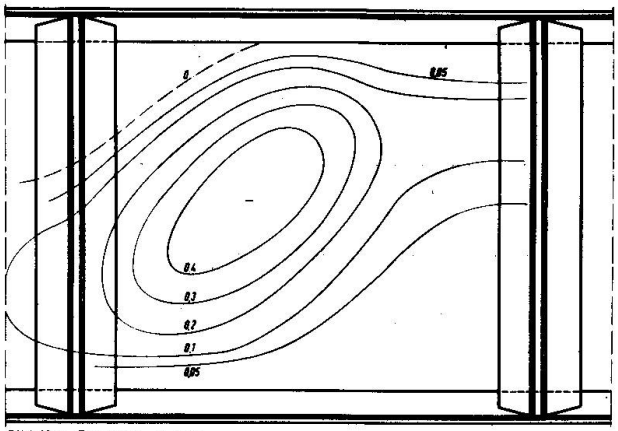

Bild 13d: Träger 6B, P=2Mp

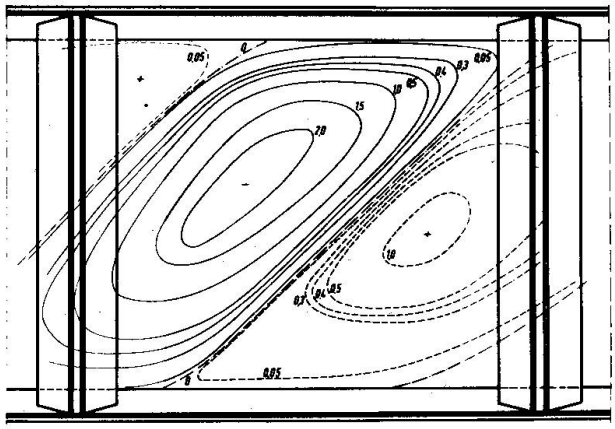

Bild 13e: Träger 6B, P=4Mp

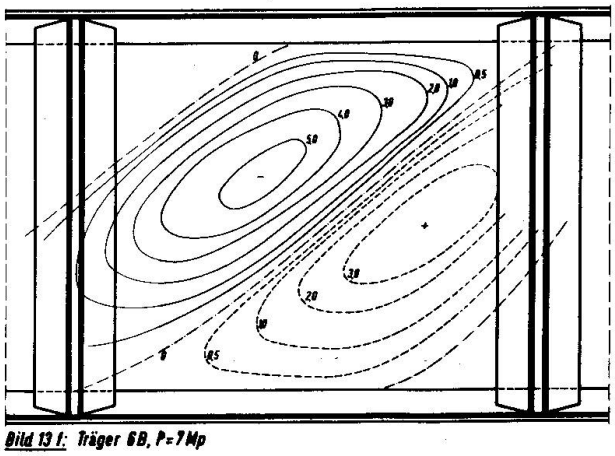

Bild 13f: Träger 6B, P=7Mp

Bild 13: Beulfiguren Feld II, Träger 6A, 6B Beultiefen in [mm]

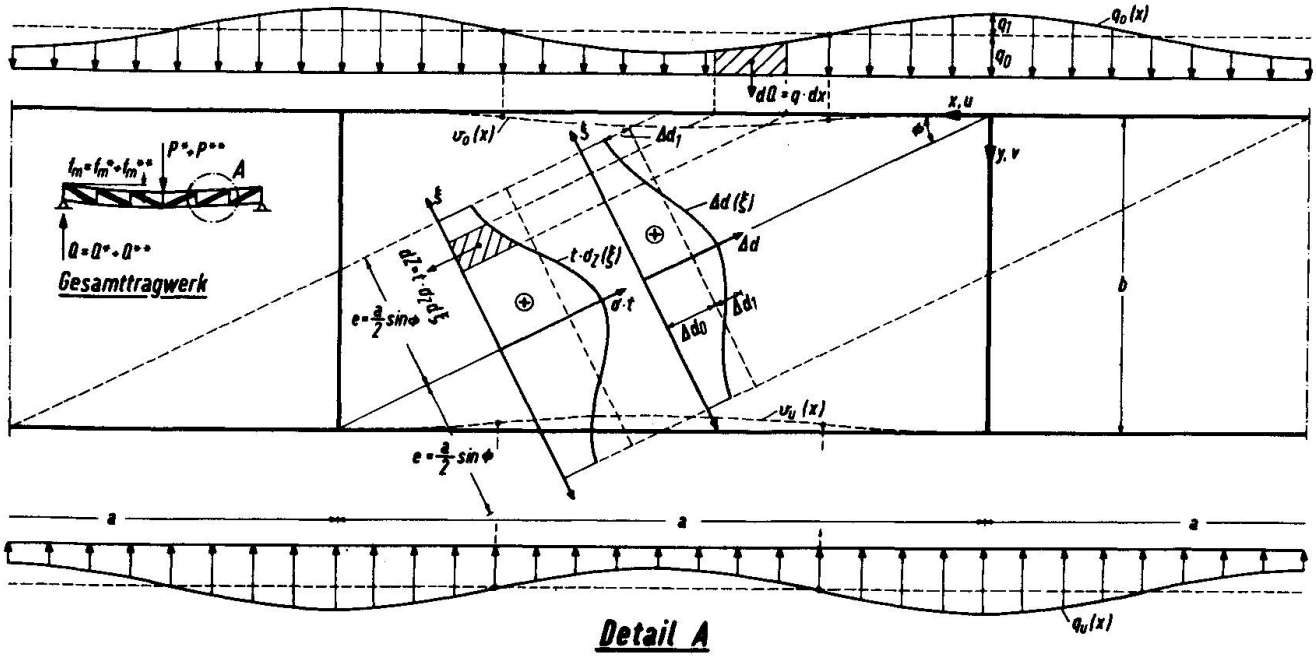

Bild 14: Kräftespiel und Verformungen an Zugfeld und Gurten für Teilbelastung Q^{++}

den Randbedingungen $v(o) = v'(o)$, $v'(a/2) = v'''(a/2)$ ergibt sich hierzu die Durchbiegungs-Funktion für die Gurte zu

$$v(x) = \frac{a^4}{24E\cdot J}\cdot q_o \left[\left(\frac{x}{a}\right)^4 - 2\cdot\left(\frac{x}{a}\right)^3 + \left(\frac{x}{a}\right)^2\right] - \frac{2}{E\cdot J}\cdot\left(\frac{a}{2\pi}\right)^4\cdot q_1\cdot\sin^2\frac{\pi\cdot x}{a} \qquad (2)$$

die mit ausreichender Genauigkeit durch die Funktion

$$v(x) = \left[C_o\cdot q_o - C_1\cdot q_1\right]\cdot\sin^2\frac{\pi\cdot x}{a} \qquad (3)$$

mit $C_o = \frac{1}{24EJ}\cdot\left(\frac{a}{2}\right)^4$ und $C_1 = \frac{1}{8EJ}\cdot\left(\frac{a}{\pi}\right)^4$ angenähert werden kann.

Ein Teil der Gurtverformung wird durch die Verkürzung der Stegblechhöhe infolge Ausbeulens kompensiert. Für das D i a g o n a l z u g f e l d ergibt sich deshalb mit

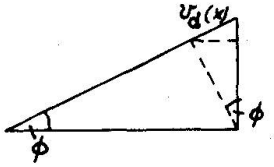

$$v_d(x) = v(x)\cdot\sin\phi$$

und $d = a/\cos\phi$ die Verformung

$$\Delta d(\xi) = \frac{\sigma_z(\xi)\cdot a}{E\cdot\cos\phi} \qquad (4)$$

die sich bei Einführung der Größe $e = \frac{1}{2}\cdot a\cdot\sin\phi$ zu (5)

$$\Delta d(\xi) = \Delta d_o + \Delta d_1 - 2\cdot\Delta d_1\cdot\sin^2\frac{\pi\cdot\xi}{2\cdot e} \tag{6}$$

umformen läßt. Hierbei resultiert Δd_1 aus den Gurtverformungen zu

$$\Delta d_1 = 2\left[C_o\cdot q_o - C_1\cdot q_1\right]\cdot\sin\phi \tag{7}$$

womit aus Formel (4) mit (6) und (7) sich die Spannung zu

$$\sigma_z(\xi) = \frac{E\cdot\cos\phi}{a}\cdot\left[\Delta d_o+2\cdot(C_o\cdot q_o-C_1\cdot q_1)\cdot\sin\phi-4\sin\phi(C_o q_o-C_1\cdot q_1)\cdot\sin^2\frac{\pi\cdot\xi}{2\cdot e}\right] \tag{8}$$

ergibt. –

In den Gleichungen (3) und (8) sind die 3 Unbekannten q_o, q_1 und Δd_o enthalten Hierzu werden die 3 Gleichgewichtsgleichungen herangezogen:

$$\int_o^{a/2} q(x)dx = \int_o^{a/2}\left[q_o+q_1(1-2\cdot\sin^2\frac{\pi x}{a})\right]dx = \frac{1}{2}\,Q^{++} \tag{9}$$

$$t\cdot\int_o^{e}\sigma_z(\xi)\cdot d\xi = \frac{1}{2}\,Q^{++}\cdot\frac{1}{\sin\phi} \tag{10}$$

Neben diesen beiden integralen Betrachtungen muß auch am Differential das Gleichgewicht $dZ = dQ/\sin\phi$ bestehen; hieraus ergibt sich nach <u>Bild 14</u> mit $dZ = t\cdot\sigma_z(\xi)\cdot d\xi$ und $dQ = q(x)\cdot dx$

$$q(x)\cdot dx = t\cdot\sigma_z(\xi)\cdot\sin^2\phi\cdot dx \tag{11}$$

Die Unbekannten ergeben sich aus den Gleichungen (9), (10)und (11) zu:

$$q_o = \frac{Q^{++}}{a}$$

$$\Delta d_o = \frac{Q^{++}\cdot a}{E\cdot t\cdot e\cdot\sin 2\phi} \tag{12}$$

$$q_1 = \frac{q_o\cdot C_o}{\frac{1}{2A\cdot\sin\phi}+C_1} \quad\text{mit}\quad A = \frac{E\cdot t\cdot\sin^2\phi\cdot\cos\phi}{a}\,.$$

Mit der so erhaltenen Querbelastung der Gurte überlagert mit der Normalkraftbeanspruchung, die aus der gesamten Beanspruchung infolge $Q = Q^{+} + Q^{++}$ und dem Biegemoment M resultiert, lassen sich für den möglichen Fall des Gurt-Versagens – A u s b i l d u n g v o n F l i e ß g e l e n k e n – Festigkeitsbetrachtungen anstellen,

dabei bereitet die wirklichkeitsnahe Erfassung des Gurtträgheitsmomentes (bei evtl. Einbeziehung einer mittragenden Breite des Steges) noch Schwierigkeiten. - Außerdem kann der weiterhin mögliche Fall des Versagens - F l i e ß e n i m B e r e i c h d e r Z u g d i a g o n a l e n - mit Hilfe der Formel (8) untersucht werden.

Die Fortsetzung der Versuche soll darüber Klarheit verschaffen, ob eine Abgrenzung der Lastanteile Q^{+} gegenüber Q^{++} zu erfolgen hat. Wie auch aus Bild 10 (τ_{xy}-Spannungen für Träger 2) des I. Berichtes zu ersehen ist, scheint die Schubtragfähigkeit des Steges mit Erreichen der kritischen Beullast ($P_{Kr}^{theor.}$) nicht erschöpft zu sein, sondern vermag sich auch noch in die Nähe der elastischen Grenzlast zu erhalten.